Journal of
Mechanics of
Materials and Structures

PREDICTION OF DRYING SHRINKAGE BEYOND THE PORE ISODEFORMATION ASSUMPTION

Olivier P. Coussy and Sébastien Brisard

Volume 4, Nº 2 February 2009

mathematical sciences publishers

JOURNAL OF MECHANICS OF MATERIALS AND STRUCTURES
Vol. 4, No. 2, 2009

PREDICTION OF DRYING SHRINKAGE BEYOND THE PORE ISODEFORMATION ASSUMPTION

OLIVIER P. COUSSY AND SÉBASTIEN BRISARD

The paper aims at assessing how, for a porous material whose pore size distribution is experimentally known, the variation in pore deformation with pore size might affect predictions of drying shrinkage. Unsaturated poroelasticity is first revisited in a general macroscopic thermodynamic framework irrespective of any morphology of the porous space. Saturation is shown to be a state function of capillary pressure governing the change in the solid-fluid interface energy; it can be experimentally obtained from a knowledge of pore size distribution only. Unsaturated poroelastic properties are then determined under three homogenization schemes: the standard Mori–Tanaka scheme, the self-consistent scheme, and the differential homogenization scheme extended to unsaturated conditions. Except for the Mori–Tanaka scheme, the function weighting the fluid pore pressure in the poroelastic constitutive equations is found to depart from the pore volume fraction the liquid occupies. As a result the pores do not deform uniformly. This departure roughly accounts for the difference in deformation between pores of different sizes and subjected to the same pressure, and it is found to significantly affect predictions of drying shrinkage, in particular for cement paste.

Drying shrinkage of water-infiltrated materials is relevant to many kinds of materials and disciplines: cement-based materials in civil engineering [Baroghel-Bouny et al. 1999], woods in the building industry [Santos 2000], plants in botany [Kozlowski and Pallardy 2002], soils in soil science [Chertkov 2002], gels in physical chemistry [Smith et al. 1995], vegetables in foods engineering [Ratti 1994], tissues in biomechanics [Gusnard and Kirschner 1977], etc. The mechanism of drying shrinkage is well known. When a porous material is subjected to an outer relative humidity lower than its initial inner relative humidity, the vapour thermodynamic imbalance forces the porous material to exchange water vapour with the outer atmosphere, so that the outer relative humidity progressively takes hold within the material. In turn liquid water simultaneously evaporates in order to maintain the vapour-liquid equilibrium. This causes the decrease of the degree of liquid saturation. The shrinkage of the porous material finally results from the lowering in liquid pressure induced by the desaturation process at the gas-liquid water interface. While the kinetics of drying is governed by transport phenomena [Mainguy et al. 2001], asymptotic drying shrinkage is governed by the outer relative humidity only, since, asymptotically, the value of the air pressure tends toward the atmospheric pressure.

The macroscopic modeling of drying shrinkage has been addressed by many authors; see [Bazant and Wittmann 1982; Coussy et al. 1998], for example. In the last decade the development of micro-poromechanics [Dormieux et al. 2006a] has provided new tools to assess the influence of microstructure

Keywords: drying, unsaturated, poroelasticity, homogenization scheme, pore size distribution, homogenization, drying shrinkage.

The authors acknowledge the support of the ATILH-CNRS research program “Porosity, Transport, Strength”.

upon drying shrinkage [Chateau and Dormieux 2002], and in particular the influence of pore shape and geometry changes [Chateau et al. 2003].

In most approaches to the mechanical behaviour of unsaturated porous materials, such as geomaterials [Lewis and Schrefler 1998; Hutter et al. 1999], and to the subsequent prediction of their drying shrinkage, the pore volume fraction occupied by a fluid is generally taken as the weighting factor for the fluid pore pressure in the constitutive equations. This approach results from the assumption that all pores (irrespective of their size) undergo the same deformation when subjected to the same pressure. Owing to their disparity in size and shape, this assumption is questionable.

The main goal of this paper is to draw attention to how the difference in deformation undergone by pores can quantitatively be taken into account in predicting drying shrinkage for a material whose pore size distribution is experimentally known. In Section 1 the poroelasticity of unsaturated porous solids is considered within a general macroscopic thermodynamic framework, irrespective of the morphology of the porous space. Saturation is shown to be a state function of the capillary pressure governing the change in the solid-fluid interface energy and can be determined from a knowledge of the pore size distribution only. In Section 2, following the methods developed in [Dormieux et al. 2006a], we determine the unsaturated poroelastic properties with the help of three homogenization schemes: the standard Mori–Tanaka scheme, the self-consistent scheme and the differential homogenization scheme extended to unsaturated conditions. Except for the Mori–Tanaka scheme, the function weigthing the fluid pore pressure in the poroelastic constitutive equations departs from the pore volume fraction that the liquid occupies. Using these homogenization schemes and adopting the experimental pore size distribution appropriate for a typical cement paste, our analysis reveals (Section 3) that this departure may significantly affect predictions of drying shrinkage and ultimately of failure for a water-infiltrated material subjected to drying.

1. Unsaturated poroelasticity

Capillary pressure curve. Consider an element of a porous solid of overall volume V, with initial porosity ϕ_0, so that its porous volume is $\phi_0 V$. For the time being, we assume that the porous solid is undeformable, so that its porosity remains constant. The porous solid, initially fully saturated by a wetting liquid denoted by subscript L, is progressively invaded by a nonwetting gas denoted by subscript G. At a given time the fractions of the porous volume $\phi_0 V$ occupied by the liquid and by the gas are S_{L} and S_{G}. We write

$$\phi_{\mathrm{L}} = \phi_0 S_{\mathrm{L}}, \quad \phi_{\mathrm{G}} = \phi_0 S_{\mathrm{G}}, \quad S_{\mathrm{L}} + S_{\mathrm{G}} = 1, \tag{1-1}$$

where ϕ_{J} is the partial porosity related to phase J (= L or G).

Assuming no hysteresis, the first and second laws of thermodynamics combine to give the isothermal incremental free energy balance

$$\mu_{\mathrm{L}}\, \mathrm{d}n_{\mathrm{L}} + \mu_{\mathrm{G}}\, \mathrm{d}n_{\mathrm{G}} - \mathrm{d}A = 0 \tag{1-2}$$

[Coussy 2004], where μ_{J} and n_{J} are respectively the chemical potential and the number of moles per unit of volume V relative to phase J, and A is the Helmholtz free energy of the whole matter contained in the volume V. The standard isothermal Gibbs–Duhem equality applied to phase J reads

$$\phi_{\mathrm{J}}\, \mathrm{d}p_{\mathrm{J}} - n_{\mathrm{J}}\, \mathrm{d}\mu_{\mathrm{J}} = 0,$$

where p_{J} is the pressure related to phase J. Let F denote the Helmholtz free energy of the system once the bulk phases L and G are removed. Owing to the additive character of energy we can write

$$F = A - (\mu_{\mathrm{L}} n_{\mathrm{L}} + \mu_{\mathrm{G}} n_{\mathrm{G}} - \phi_{\mathrm{L}} p_{\mathrm{L}} - \phi_{\mathrm{G}} p_{\mathrm{G}}) . \tag{1-3}$$

The three last equations combine to give

$$p_{\mathrm{L}}\, \mathrm{d}\phi_{\mathrm{L}} + p_{\mathrm{G}}\, \mathrm{d}\phi_{\mathrm{G}} - \mathrm{d}F = 0. \tag{1-4}$$

Since in (1-3) the bulk liquid and gas phases have been removed and the porous solid is assumed to be undeformable, the free energy F reduces to the surface energy of the interfaces between the phases and the solid matrix. Denoting by U the surface energy of these interfaces per unit volume, we write

$$F = \phi_0 U. \tag{1-5}$$

Substituting (1-1) and (1-5) in (1-4) we get

$$p_{\mathrm{G}} - p_{\mathrm{L}} = -\frac{\mathrm{d}U}{\mathrm{d}S_{\mathrm{L}}}, \tag{1-6}$$

which shows that the liquid saturation S_{L} is a state function of the capillary pressure $p_{\mathrm{G}} - p_{\mathrm{L}}$. We write

$$S_{\mathrm{L}} = \varpi\, (p_{\mathrm{G}} - p_{\mathrm{L}}) , \tag{1-7}$$

where ϖ describes the so-called capillary curve. The macroscopic capillary curve can receive a simple microscopic interpretation at the pore scale. At that scale the mechanical equilibrium of the current gas-liquid interface is governed by the Laplace law according to

$$p_{\mathrm{G}} - p_{\mathrm{L}} = \frac{2\gamma_{\mathrm{GL}}}{r}, \tag{1-8}$$

where γ_{LG} is the energy per unit of surface of the gas-liquid interface and r is the mean curvature radius. As illustrated in Figure 1 for a cement paste, standard porosimetry provides the cumulated porous volume fraction $S\,(r)$ of pores having a pore entry radius smaller than r. For a given value of the capillary pressure $p_{\mathrm{G}} - p_{\mathrm{L}}$, pores having an entry radius smaller than the one given by (1-8) will still remain filled with liquid, while pores with larger entry radius will be invaded by the gas. As a consequence we write

$$S_{\mathrm{L}} = S(r). \tag{1-9}$$

Combining (1-8) and (1-9) we get

$$S_{\mathrm{L}} = S\left(\frac{2\gamma_{\mathrm{GL}}}{p_{\mathrm{G}} - p_{\mathrm{L}}}\right), \tag{1-10}$$

which provides an explicit determination of the capillary curve.

Unsaturated state equations of poroelasticity. Now consider a deformable porous solid and denote by σ_{ij} and ε_{ij} the stress and strain components. The free energy balance (1-4) is extended to

$$\sigma_{ij}\, \mathrm{d}\varepsilon_{ij} + p_{\mathrm{L}}\, \mathrm{d}\phi_{\mathrm{L}} + p_{\mathrm{G}}\, \mathrm{d}\phi_{\mathrm{G}} - \mathrm{d}F = 0, \tag{1-11}$$

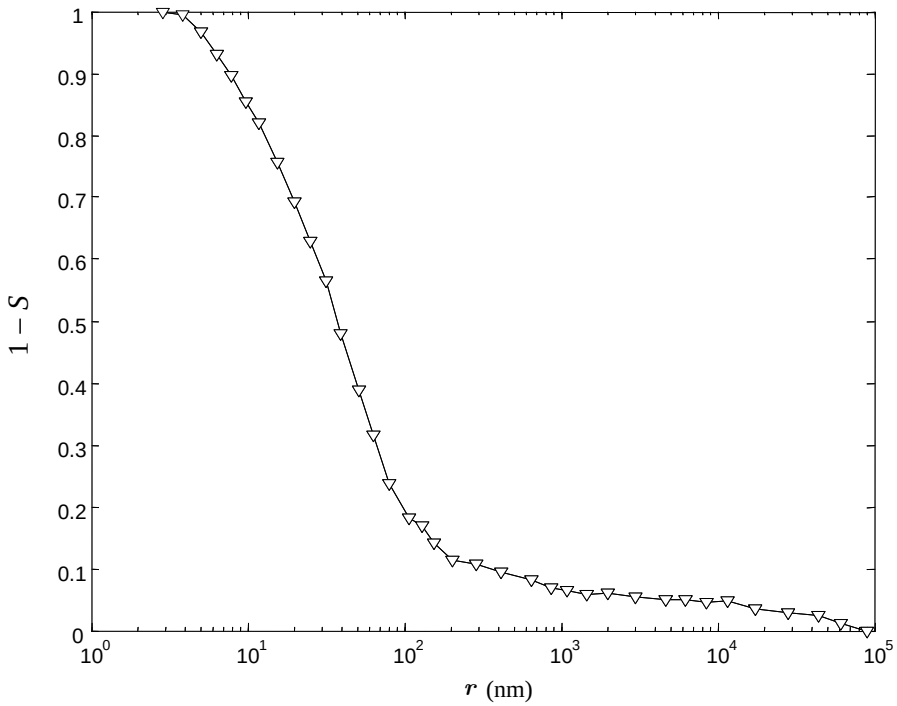

Figure 1. Cumulative pore volume fraction $1 - S(r)$ of pores having a pore entry radius greater than r for a typical cement paste (extracted from [Huang and Feldman 1985]).

where $\sigma_{ij}\,\mathrm{d}\varepsilon_{ij}$ accounts for the strain work. Since the porous space now deforms, instead of (1-1) we write

$$\phi_{\mathrm{L}} = \phi_0 S_{\mathrm{L}} + \varphi_{\mathrm{L}}, \quad \phi_{\mathrm{G}} = \phi_0 S_{\mathrm{G}} + \varphi_{\mathrm{G}}, \quad S_{\mathrm{L}} + S_{\mathrm{G}} = 1, \tag{1-12}$$

where φ_{J} accounts for the change in the partial porosity ϕ_{J} due to deformation only. In contrast to the standard Eulerian configuration referring to the current deformed configuration, as recently introduced in [Coussy 2007], the saturation S_{J} can be regarded as a Lagrangian saturation related to phase J, since it refers to the undeformable configuration. More precisely, starting from full liquid saturation, $\phi_0 S_{\mathrm{L}} V$ is the volume in the undeformable configuration whose solid walls will still be wetted in the current deformed configuration [Coussy 2007]. This is sketched in Figure 2 for two distinct current deformed configurations, the undeformed reference configuration pertaining to liquid saturated conditions at zero pressure p_{L}.

With regard to the undeformable porous solid, the free energy F of the deformable system obtained by removing the bulk phases L and G now splits into the surface energy $\phi_0 U$ associated with the interfaces, and the elastic energy Ψ_{S} stored in the deformable solid matrix. Accordingly expression (1-5) transforms into

$$F = \phi_0 U + \Psi_{\mathrm{S}}. \tag{1-13}$$

Substitution of (1-12) and (1-13) into (1-11) yields

$$\sigma_{ij}\,\mathrm{d}\varepsilon_{ij} + p_{\mathrm{L}}\,\mathrm{d}\varphi_{\mathrm{L}} + p_{\mathrm{G}}\,\mathrm{d}\varphi_{\mathrm{G}} - \mathrm{d}\Psi_{\mathrm{S}} - \phi_0\big((p_{\mathrm{G}} - p_{\mathrm{L}})\,\mathrm{d}S_{\mathrm{L}} + \mathrm{d}U\big) = 0. \tag{1-14}$$

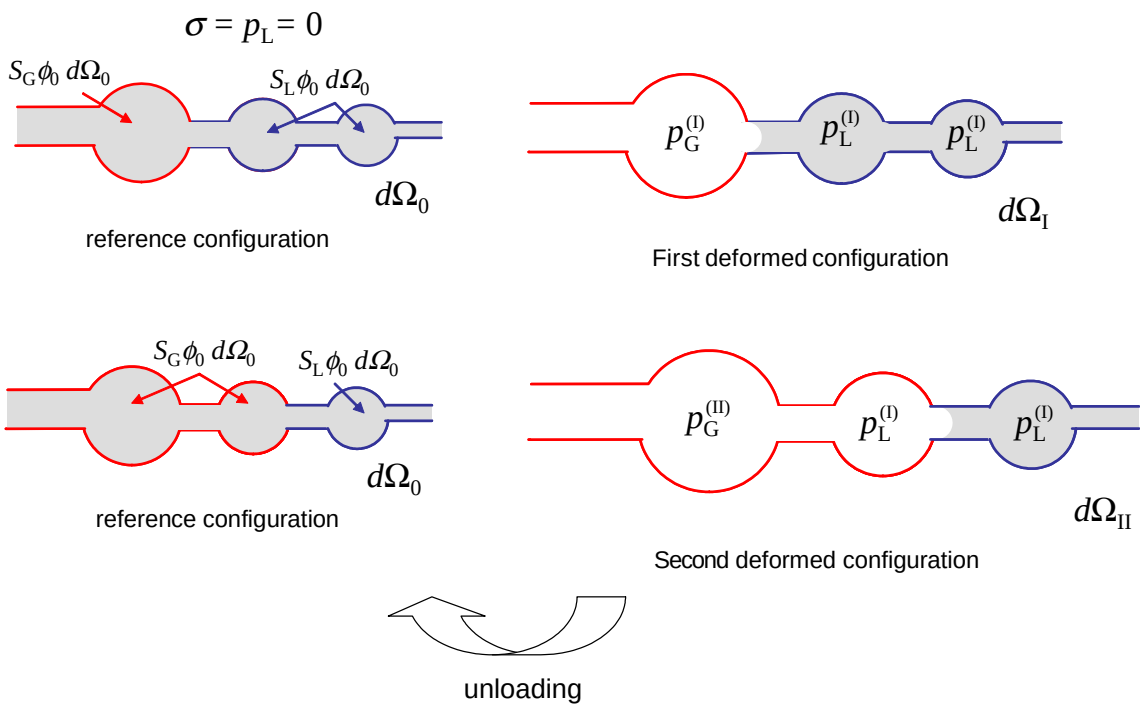

Figure 2. Unlike the case of disconnected porous networks, for a porous solid formed of connected pores embedded in a solid matrix the Lagrangian saturation S_J does not remain constant, since either fluid, the gas G or the liquid L, can invade the porous solid or recede from it.

When the porous solid is deformable, in contrast to the previous section, even when S_L is held constant, U can change because it is affected by the deformation of the solid-fluid interface. The change in U is then due to the work produced by the pressure difference exerted on the solid-fluid interface and made possible by the solid-fluid surface energy γ_{SG} or γ_{SL}. However, because of the low values of γ_{SG} and γ_{SL} compared to the elastic energy, as the liquid saturation changes during the process of invasion by the gas, the change in U is mainly due to the creation of new interfaces between the phases. According to the analysis of the previous section, U can then still be considered as a function of the liquid saturation S_L only. Conversely, if we assume infinitesimal elastic deformations of the porous solid, the elastic energy Ψ_S will be slightly affected by the variation $\mathrm{d}S_L$ of the liquid saturation. As a result, (1-14) allows us to conclude that (1-5) will still hold to a good approximation, while the free energy balance related to the deformable porous solid obtained by removing the interfaces is

$$\sigma_{ij}\,\mathrm{d}\varepsilon_{ij} + p_L\,\mathrm{d}\varphi_L + p_G\,\mathrm{d}\varphi_G - \mathrm{d}\Psi_S = 0, \tag{1-15}$$

from which we derive

$$\sigma_{ij} = \frac{\partial \Psi_S}{\partial \varepsilon_{ij}}, \quad p_L = \frac{\partial \Psi_S}{\partial \varphi_L}, \quad p_G = \frac{\partial \Psi_S}{\partial \varphi_G}. \tag{1-16}$$

Letting $W_S = \sigma_{ij}\varepsilon_{ij} + \varphi_L p_L + \varphi_G p_G - \Psi_S$ be the Legendre transform of Ψ_S with regard to φ_J we alternatively get

$$\varepsilon_{ij} = \frac{\partial W_S}{\partial \sigma_{ij}}, \quad \varphi_L = \frac{\partial W_S}{\partial p_L}, \quad \varphi_G = \frac{\partial W_S}{\partial p_G}. \tag{1-17}$$

In the context of both infinitesimal deformation, and restricting to linear isotropic poroelasticity, the expression of the elastic energy of the solid matrix, $W_S = \Psi_S$, is

$$W_S = \frac{1}{2K}(\sigma + b_L p_L + b_G p_G)^2 + \frac{1}{2N_{LL}} p_L^2 + \frac{1}{N_{LG}} p_L p_G + \frac{1}{2N_{GG}} p_G^2 + \frac{1}{4G} s_{ij} s_{jk}, \tag{1-18}$$

where $\sigma = \sigma_{kk}/3$ and s_{ij} represent the mean stress and the components of the deviatoric stress tensor. Letting $\varepsilon = \varepsilon_{kk}$ be the volumetric strain and substituting (1-18) in (1-17) we finally get

$$\sigma = K\varepsilon - b_L p_L - b_G p_G, \qquad s_{ij} = 2Ge_{ij}, \tag{1-19}$$

$$\varphi_L = b_L \varepsilon + p_L/N_{LL} + p_G/N_{LG}, \tag{1-20}$$

$$\varphi_G = b_G \varepsilon + p_L/N_{LG} + p_G/N_{GG}. \tag{1-21}$$

K and G are therefore identified as the bulk modulus and the shear modulus of the dry porous solid with no internal pore pressures.

When $p_L = p_G$ we must retrieve the saturated case so that we have [Coussy 2004]

$$b_L + b_G = b = 1 - \frac{K}{k_S} \quad \text{and} \quad \frac{1}{N_{LL}} + \frac{2}{N_{LG}} + \frac{1}{N_{GG}} = \frac{1}{N} = \frac{b - \phi_0}{k_S}, \tag{1-22}$$

where b and N are the poroelastic properties of the porous solid with uniform pore pressure, while k_S is the bulk modulus of the solid matrix assumed to be homogeneous. Using mesoscopic-macroscopic considerations [Coussy 1991; 2007] or more refined upscaling methods [Dormieux et al. 2006a], it can further be shown that

$$\frac{1}{N_{JJ}} + \frac{1}{N_{LG}} = \frac{b_J - \phi_0 S_J}{k_S}. \tag{1-23}$$

Provided that k_S is known, these relations are independent of the porous solid considered. In contrast, separate expressions for the poroelastic properties K, G, b_J and N_{JK} as functions of the porosity ϕ_0 and saturation S_J require specific information on the porous solid considered.

2. Estimates of the unsaturated poroelastic properties

Pore isodeformation. The first relation in (1-22) shows that b_L and b_G are not independent and allows us to introduce a Bishop-like parameter χ (see [Bishop and Blight 1963]) depending on the liquid saturation $S_L$and such that

$$b_L = b\chi(S_L), \quad b_G = b\big(1 - \chi(S_L)\big). \tag{2-1}$$

The explicit determination of function $\chi(S_L)$ requires additional information. One assumption, sometimes made implicitly [Coussy 2004] or explored explicitly [Chateau and Dormieux 2002; Dormieux et al. 2006a; Coussy 2007], is the isodeformation of the porous volumes respectively occupied by the

liquid and the gas in the absence of any pore pressure. This assumption amounts to writing

$$\frac{\varphi_{\mathrm{L}}}{\phi_0 S_{\mathrm{L}}} = \frac{\varphi_{\mathrm{G}}}{\phi_0 S_{\mathrm{G}}} \quad \text{when } p_{\mathrm{L}} = p_{\mathrm{G}} = 0. \tag{2-2}$$

Substitution of (2-2) in (1-20) and (1-21) provides

$$\frac{b_{\mathrm{L}}}{S_{\mathrm{L}}} = \frac{b_{\mathrm{G}}}{S_{\mathrm{G}}}. \tag{2-3}$$

Substituting (2-3) in $(1\text{-}22)_1$ we finally get the simple identifications

$$b_{\mathrm{J}} = bS_{\mathrm{J}}, \quad \chi = S_{\mathrm{L}}. \tag{2-4}$$

From (1-23) and (2-4) it can easily be shown that the porous volumes occupied by the liquid and the gas would still deform equally if they are subjected to the same pressure.

Mori–Tanaka and self-consistent schemes. When the pore isodeformation assumption is relevant, we are left with the determination of the bulk modulus K and the shear modulus G as functions of the porosity ϕ_0. This can be achieved using upscaling procedures, the details of which we cannot go into here; we will only recall well known results in view of their further application to the analysis of drying shrinkage. (For a comprehensive and fruitful application of micromechanics to porous materials, see [Dormieux et al. 2006a].)

Since the overall volumetric strain ε is the averaged volumetric strain, we can write, letting ε_{S} be the volumetric strain of the solid matrix,

$$\varepsilon = (1-\phi_0)\varepsilon_{\mathrm{S}} + \varphi_{\mathrm{L}} + \varphi_{\mathrm{G}}. \tag{2-5}$$

The variation of volume $\varphi_{\mathrm{J}} V$ of a spherical void of initial volume $\phi_0 S_{\mathrm{J}} V$, which is embedded within an elastic matrix with k and g as bulk and shear moduli and which is subjected to the pore pressure p_{J}, can be expressed in the form

$$\frac{\varphi_{\mathrm{J}}}{\phi_0 S_{\mathrm{J}}} = \left(1 + \frac{3k}{4g}\right)\varepsilon_0 + \frac{3}{4g} p_{\mathrm{J}}, \tag{2-6}$$

where ε_0 is the volumetric strain prescribed at infinity. If the spherical void is replaced by a spherical solid inclusion with k_{S} as bulk modulus, the volumetric strain ε_{S} of the latter is given by

$$\varepsilon_{\mathrm{S}} = \frac{3k+4g}{3k_{\mathrm{S}}+4g}\varepsilon_0. \tag{2-7}$$

Substitution of (2-6) for J = L and G and (2-7) into (2-5) yields ε_0 in the form

$$\varepsilon_0 = \frac{3k_{\mathrm{S}}+4g}{3\phi_0 k_{\mathrm{S}}+4g} \times \frac{4g}{3k+4g}\left(\varepsilon - \frac{3\phi_0}{4g}(S_{\mathrm{L}} p_{\mathrm{L}} + S_{\mathrm{G}} p_{\mathrm{G}})\right). \tag{2-8}$$

In turn, substituting (2-8) in (2-6) we recover the constitutive equations (1-20) and (1-21) of unsaturated poroelasticity and the associated relations (1-22)–(1-23), but now with the benefit of the new relations

$$b_{\mathrm{J}} = bS_{\mathrm{J}}, \quad K = (1-\phi_0)\,\frac{4k_{\mathrm{S}}g}{3\phi_0 k_{\mathrm{S}} + 4g}, \tag{2-9}$$

$$\frac{1}{N_{\mathrm{JJ}}} = S_{\mathrm{J}}^2\left(\frac{1}{N} - \frac{3\phi_0}{4g}\right) + \frac{3\phi_0 S_{\mathrm{J}}}{4g}, \quad \frac{1}{N_{\mathrm{LG}}} = S_{\mathrm{L}}S_{\mathrm{G}}\left(\frac{1}{N} - \frac{3\phi_0}{4g}\right).$$

These relations agree with those given in [Dormieux et al. 2006a].

The homogenization schemes differ by the choice of the embedding medium with elastic properties k and g. The Mori–Tanaka scheme consists in choosing the solid matrix as the embedding medium, that is, $k = k_{\mathrm{S}}$ and $g = g_{\mathrm{S}}$ so that $\varepsilon_0 = \varepsilon_{\mathrm{S}}$. The self-consistent scheme consists in choosing as the embedding medium the porous solid whose poroelastic properties we seek, that is, $k = K$ and $g = G$. The determination of the relations providing the missing relation involving the shear modulus G is much less straightforward, since it corresponds to prescribing at infinity the deviatoric strain instead of the volumetric strain [Dormieux et al. 2006a]. We limit ourselves to recalling the final result:

$$G = (1-\phi_0)\,\frac{(9k+8g)\,g_{\mathrm{S}}}{9k\left(1+\frac{2}{3}\phi_0 g_{\mathrm{S}}/g\right) + 8g\left(1+\frac{3}{2}\phi_0 g_{\mathrm{S}}/g\right)}. \tag{2-10}$$

In view of the explicit determination of K and G, further calculations lead us to rewrite (2-9) and (2-10), with $k = K$ and $g = G$, in the more convenient form

$$\frac{K}{k_{\mathrm{S}}} = 1 - \phi_0\,(1 + 3K/4G)\,, \quad \frac{G}{g_{\mathrm{S}}} = 1 - 5\phi_0\,\frac{1+4G/3K}{3+8G/3K}. \tag{2-11}$$

Letting

$$A = \frac{4G}{3K} = 2\frac{1-2\nu}{1+\nu}, \quad a_{\mathrm{S}} = \frac{4g_{\mathrm{S}}}{3k_{\mathrm{S}}} = 2\frac{1-2\nu_{\mathrm{S}}}{1+\nu_{\mathrm{S}}}, \tag{2-12}$$

where ν and ν_{S} stand for the Poisson coefficients, relations (2-11) combine to give

$$2(1-\phi_0)\left(A - \frac{\phi_0}{1-\phi_0}\right)^2 + \big(3 - \phi_0 - (2-5\phi_0)a_{\mathrm{S}}\big)\left(A - \frac{\phi_0}{1-\phi_0}\right) - 3\frac{1-2\phi_0}{1-\phi_0}a_{\mathrm{S}} = 0. \tag{2-13}$$

Retaining the solution of (2-13) that matches the solution $\phi_0/\,(1-\phi_0)$ for $k_{\mathrm{S}} \to \infty$, namely $a_{\mathrm{S}} = 0$, we finally find

$$A - \frac{\phi_0}{1-\phi_0} = \frac{(2-5\phi_0)a_{\mathrm{S}} - 3 + \phi_0 + \sqrt{\big(3-\phi_0-(2-5\phi_0)a_{\mathrm{S}}\big)^2 + 24a_{\mathrm{S}}(1-2\phi_0)}}{4(1-\phi_0)}, \tag{2-14}$$

which in turn can be substituted in the relation $\dfrac{K}{g_{\mathrm{S}}} = \dfrac{4G}{3Ag_{\mathrm{S}}}$ and in $(2\text{-}11)_2$.

Beyond pore isodeformation. The first relation in (2-9), which is identical to (2-4), holds irrespective of the choice of the embedding medium. This is because the standard upscaling schemes considered here are all based on the solution to the problem of a single inclusion embedded in an infinite medium. Therefore neither absolute length scales (since the embedding medium is infinite) nor relative ones (since

only one inclusion is considered at a time) can be introduced. Thus no scale effect associated with the pore size distribution can arise from these models.

With a view toward accounting for this scale effect, we start by considering only two sizes of pores, denoted respectively by subscript G (the larger pores occupied by the nonwetting gas) and subscript L (smaller pores occupied by the wetting liquid), in conformity with the analysis we carried out in the first section.

We assume scale separation between the smaller and larger pores, which is clearly a convenient oversimplification, since the smallest pores occupied by the gas have a size comparable with the largest pores occupied by the liquid. Within this assumption, the larger pores are embedded in a porous matrix. At this scale we have

$$b_{\mathrm{G}} = 1 - \frac{K}{\kappa_{\mathrm{G}}} \quad \text{and} \quad \frac{1}{N_{\mathrm{GG}}} = \frac{b_{\mathrm{G}} - \phi_0 S_{\mathrm{G}}}{\kappa_{\mathrm{G}}}, \tag{2-15}$$

where κ_{G} is the bulk modulus of the porous solid matrix consisting of the original solid matrix and of the smaller pores forming the porous volume at pressure p_{L}. The porosity ϕ_0^{G} of this porous solid matrix is the ratio of the porous volume at pressure p_{L} to the overall volume from which we remove the porous volume at pressure p_{G}. Accordingly we write

$$\phi_0^{\mathrm{G}} = \frac{\phi_0 S_{\mathrm{L}}}{1 - \phi_0 S_{\mathrm{G}}}. \tag{2-16}$$

From the general relation (1-23) the other poroelastic properties are then derived in sequence:

$$b_{\mathrm{L}} = b - b_{\mathrm{G}} = \frac{K}{\kappa_{\mathrm{G}}} - \frac{K}{k_{\mathrm{S}}}, \qquad \frac{1}{N_{\mathrm{LG}}} = \frac{b_{\mathrm{G}} - \phi_0 S_{\mathrm{G}}}{k_{\mathrm{S}}} - \frac{b_{\mathrm{G}} - \phi_0 S_{\mathrm{G}}}{\kappa_{\mathrm{G}}}, \qquad \frac{1}{N_{\mathrm{LL}}} = \frac{b_{\mathrm{L}} - \phi_0 S_{\mathrm{L}}}{k_{\mathrm{S}}} - \frac{1}{N_{\mathrm{LG}}}. \tag{2-17}$$

The assessment of the poroelastic properties requires the determination of κ_{G}. One might think of carrying out this determination using the Mori–Tanaka scheme of the previous section, the expression for κ_{G} being derived from (2-9)$_2$ in the form

$$\kappa_{\mathrm{G}} = \left(1 - \phi_0^{\mathrm{G}}\right) \frac{4 k_{\mathrm{S}} g_{\mathrm{S}}}{3\phi_0^{\mathrm{G}} k_{\mathrm{S}} + 4 g_{\mathrm{S}}}. \tag{2-18}$$

However, when combining (2-16)–(2-18) it can easily be checked that relations (2-9) are preserved. This is an unexpected result, for it can be shown that the two populations of pores do not sustain the same volumetric strain when subjected to the same pressure. However, the macroscopic shrinkage turns out to be equal to what it would be had the pore isodeformation assumption been valid ($b_{\mathrm{J}} = b S_{\mathrm{J}}$).

Turning our attention to the self-consistent scheme, we have

$$\begin{gathered} K = (1 - \phi_0) \frac{4 k_{\mathrm{S}} G}{3\phi_0 k_{\mathrm{S}} + 4G}, \quad \kappa_{\mathrm{G}} = \left(1 - \phi_0^{\mathrm{G}}\right) \frac{4 k_{\mathrm{S}} \gamma_{\mathrm{G}}}{3\phi_0^{\mathrm{G}} k_{\mathrm{S}} + 4\gamma_{\mathrm{G}}} \\ \gamma_{\mathrm{G}} = \left(1 - \phi_0^{\mathrm{G}}\right) \frac{(9\kappa_G + 8\gamma_G)\, g_{\mathrm{S}}}{9\kappa_G\left(1 + \frac{2}{3}\phi_0^{\mathrm{G}} g_{\mathrm{S}}/\gamma_{\mathrm{G}}\right) + 8\gamma_{\mathrm{G}}\left(1 + \frac{3}{2}\phi_0^{\mathrm{G}} g_{\mathrm{S}}/\gamma_{\mathrm{G}}\right)}, \end{gathered} \tag{2-19}$$

where γ_{G} is the shear modulus associated with κ_{G}. Explicit expressions for κ_{G} and γ_{G} can be obtained with the help of the same procedure that led to (2-14) in the previous section. Substituting (2-19) in

(2-15)$_1$ and (2-17)$_1$, while also using (2-16), we obtain

$$b_{\mathrm{G}} = b + \phi_0 S_{\mathrm{L}} \frac{1 - G/\gamma_{\mathrm{G}}}{\phi_0 + 4G/3k_{\mathrm{S}}} \quad \text{and} \quad b_{\mathrm{L}} = bS_{\mathrm{L}} - \phi_0 S_{\mathrm{L}} \frac{1 - G/\gamma_{\mathrm{G}}}{\phi_0 + 4G/3k_{\mathrm{S}}}. \tag{2-20}$$

Since $b = 1 - K/k_{\mathrm{S}}$, the expression (2-19) for K can be combined with (2-20) to give the following expression for the quantity χ of (2-1):

$$\chi = S_{\mathrm{L}} \left(\frac{G/\gamma_{\mathrm{G}} + 4G/3k_{\mathrm{S}}}{1 + 4G/3k_{\mathrm{S}}} \right). \tag{2-21}$$

As a consequence, relation (2-4) no longer holds, so the pores do not undergo the same deformation. The remaining poroelastic properties N_{JK} are obtained by substituting (2-18)–(2-20) into (2-17).

The third homogenization scheme we consider is the differential scheme. Whereas the use of this scheme is well known to provide assessments of the elastic properties K and G of a porous solid, to the authors' knowledge it has never been used for the assessment of unsaturated poroelastic properties, and thereby for the prediction of the drying shrinkage of a porous solid. As sketched in Figure 2, the original idea of the differential scheme consists in progressively introducing the porosity by infinitesimal volume fractions according to an iterative procedure. At a given stage of the iterative procedure the porosity $\phi_0 S$ has already been introduced. The next step consists in removing a new volume fraction $\mathrm{d}f_0$ out of the porous solid and replacing it by the same volume of pores. Since the fraction $\phi_0 S$ of $\mathrm{d}f_0$ already consisted of pores, the incremental porosity $\phi_0 \mathrm{d}S$ finally created is given by

$$\mathrm{d}f_0 = \frac{\phi_0 \, \mathrm{d}S}{1 - \phi_0 S}. \tag{2-22}$$

The removal of the fraction $\mathrm{d}f_0$ has transformed the current bulk and shear moduli κ and γ in the new moduli $\kappa + \mathrm{d}\kappa$ and $\gamma + \mathrm{d}\gamma$, which can be computed as those of a porous solid of porosity $\mathrm{d}f_0$ whose solid matrix has κ and γ as bulk and shear moduli. Accordingly, in the left-hand side of (2-9)$_2$ and in (2-10), we replace K and G by $\kappa + \mathrm{d}\kappa$ and $\gamma + \mathrm{d}\gamma$, while on the right-hand side we replace k_{S}, g_{S} and ϕ_0 by κ, γ and $\mathrm{d}f_0$. Retaining only the terms of main order with regard to the infinitesimals $\mathrm{d}\kappa$, $\mathrm{d}\gamma$ and $\mathrm{d}S$, we finally get

$$\frac{\mathrm{d}\kappa}{\kappa} = -\frac{\phi_0 \, \mathrm{d}S}{1 - \phi_0 S} \left(1 + \frac{1}{a} \right), \quad \frac{\mathrm{d}\gamma}{\gamma} = -\frac{5\phi_0 \mathrm{d}S}{1 - \phi_0 S} \times \frac{1 + a}{3 + 2a}, \tag{2-23}$$

where

$$a = \frac{4\gamma}{3\kappa}. \tag{2-24}$$

Integrating (2-23) and (2-24) over κ from k_{S} to κ_{G}, over a from $a_{\mathrm{S}} = \dfrac{4g_{\mathrm{S}}}{3k_{\mathrm{S}}}$ to $a_{\mathrm{G}} = \dfrac{4g_{\mathrm{G}}}{3k_{\mathrm{G}}}$, and over S from 0 to $S_{\mathrm{L}} = 1 - S_{\mathrm{G}}$, we obtain

$$\frac{\kappa_{\mathrm{G}}}{k_{\mathrm{S}}} = \frac{|1 - a_{\mathrm{G}}|^{5/3}}{|1 - a_{\mathrm{S}}|^{5/3}} \frac{a_{\mathrm{S}}}{a_{\mathrm{G}}}; \quad \frac{|1 - a_{\mathrm{G}}|^5}{1 + a_{\mathrm{G}}} = \frac{|1 - a_{\mathrm{S}}|^5}{1 + a_{\mathrm{S}}} (1 - \phi_0 S_{\mathrm{L}})^6, \tag{2-25}$$

while the expression for the shear modulus γ_{G} is known through the relation $\gamma_{\mathrm{G}} = 3\kappa_{\mathrm{G}} a_{\mathrm{G}}/4$. The overall properties are then determined by simultaneously letting $\kappa_{\mathrm{G}} = K$ and $a_{\mathrm{G}} = 4G/3K$ in (2-25)$_1$ and letting $a_{\mathrm{G}} = 4G/3K$ and $S_{\mathrm{L}} = 1$ in (2-25)$_2$. For a given value of $S_{\mathrm{L}} = 1 - S_{\mathrm{G}}$ the unsaturated poroelastic properties b_{J} and N_{JK} are then derived by combining relations (2-25), (2-15) and (2-17).

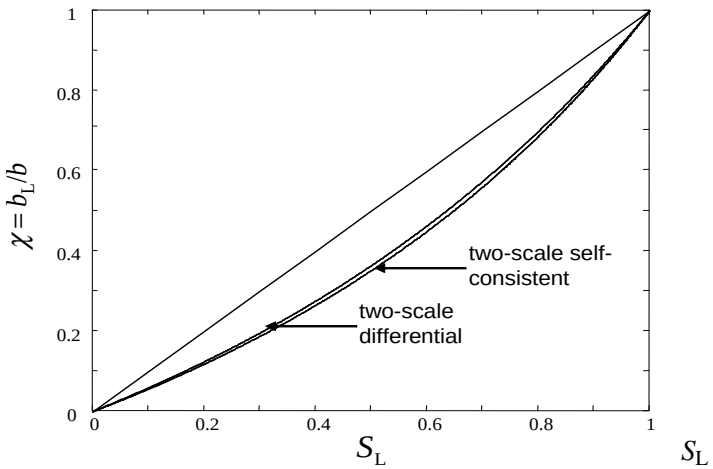

Figure 3. Bishop parameter $\chi = b_L/b$ versus liquid saturation S_L under three homogenization schemes. For the two-step self-consistent and differential schemes, χ departs from S_L, showing that pores of different sizes do not deform equally under these schemes.

Although no simple expression can be obtained when χ is defined by (2-1), as was the case for the previous two-scale self-consistent scheme, one can show that small and large pores do not undergo the same deformation when subjected to the same pressure; yet, in contrast with Mori–Tanaka's approach, (2-4) no longer holds. Figure 3 plots $\chi = b_L/b$ against S_L for the Mori–Tanaka scheme ($\chi = b_L/b = S_L$), for the two-scale self-consistent scheme and for the differential scheme. For the two-scale self-consistent and differential schemes the ratio $\chi = b_L/b$ exhibits a significant lower value than the liquid saturation S_L, which is the expression of b_L/b associated with pore isodeformation. In Figure 4 we plot the poroelastic

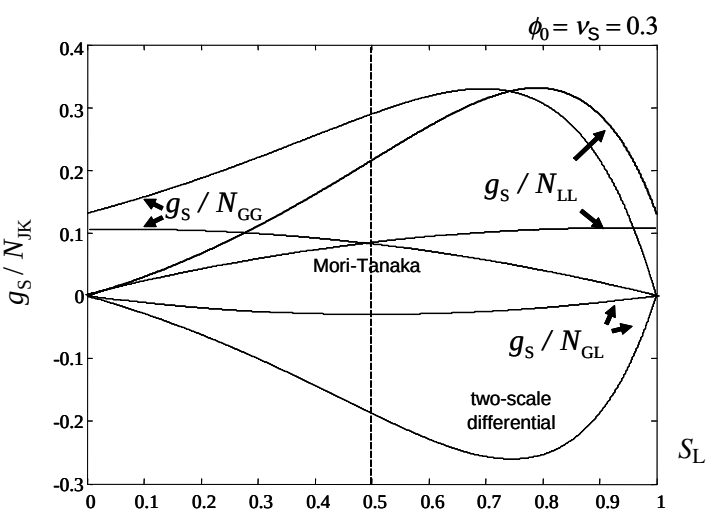

Figure 4. Poroelastic coupling property N_{JK} normalized by solid matrix shear modulus g_S versus liquid saturation for Mori–Tanaka and two-scale differential schemes.

coupling properties g_S/N_{JK} against S_L for the Mori–Tanaka scheme and the differential scheme. In the differential scheme, the coupling properties g_S/N_{JK} are not symmetric with regard to the line $S_L = \frac{1}{2}$. The properties g_S/N_{LL} and g_S/N_{GL} reach their maximum value for larger values than $S_L = \frac{1}{2}$, and the opposite holds for g_S/N_{GG}.

3. Drying shrinkage

The drying history of a water-infiltrated porous material is driven by Kelvin's law

$$p_L - p_{atm} = \frac{RT}{v_L} \ln h_R, \tag{3-1}$$

where R is the constant of ideal gases, T the temperature and v_L the water molar volume; h_R is the relative humidity, that is, the ratio p_V/p_{VS} of the vapour pressure p_V and the saturating vapour pressure p_{VS} that would prevail over liquid water at atmospheric pressure. At equilibrium the air pressure within the porous material is atmospheric. With $p_{atm} = p_G$ Kelvin's law and (1-10) combine to give

$$S_L = S\left(-\frac{2v_L\gamma_{GL}/RT}{\ln h_R}\right). \tag{3-2}$$

This captures the fact that the pore entry radius, and consequently the liquid saturation, have to adjust to the current relative humidity in order for the confined liquid water to remain in thermodynamic equilibrium with the current vapour pressure imposed by the current relative humidity. This is accompanied by a depressurization of liquid water, which in turn provokes drying shrinkage.

Consider then a stress-free drying process so that $\sigma = 0$, starting from a reference initial state where the porous material is saturated ($S_L = 1$), the pore pressure is atmospheric ($p_L = p_{atm}$) and the relative humidity is 100%. With regard to a zero pore pressure state, the deformation ε_0 related to the drying initial state is provided by substituting the initial conditions in (1-19) with $b_L = b$ and $b_G = 0$ so that

$$\varepsilon_0 = \frac{bp_{atm}}{K}. \tag{3-3}$$

When the relative humidity is lowered below 100% and the gas pressure is maintained at atmospheric pressure p_{atm} a drying shrinkage $\varepsilon_{drying} = \varepsilon - \varepsilon_0$ is observed and an associated extra elastic energy W_{drying} is stored whose respective intensity are obtained by substituting $\sigma = 0$, (2-1), (3-1) and (3-3) in (1-19) and (1-18). We get

$$\varepsilon_{drying} = -\frac{b\chi}{K}(p_G - p_L) = \frac{b\chi}{K}\frac{RT}{v_L}\ln h_R; \qquad W_{drying} = \left(\frac{b^2\chi^2}{2K} + \frac{1}{2N_{LL}}\right)\left(\frac{RT}{v_L}\ln h_R\right)^2. \tag{3-4}$$

Under a specific homogenization scheme, the poroelastic properties b, K, χ and N_{LL} are then known as functions of the porosity ϕ_0, the current liquid saturation S_L and the matrix elastic properties k_S and g_S. In addition the current liquid saturation S_L is known through (3-2) as a function of the current relative humidity h_R and the pore size distribution. Adopting for the latter the data reported in Figure 1, we have plotted ε_{drying} and W_{drying} against S_L in Figure 5, top, for the various homogenization schemes explored in this paper. Drying shrinkage exhibits a maximum in absolute value, achieved when the decrease in liquid pressure induced by the decrease in relative humidity is exactly compensated by a decrease in the

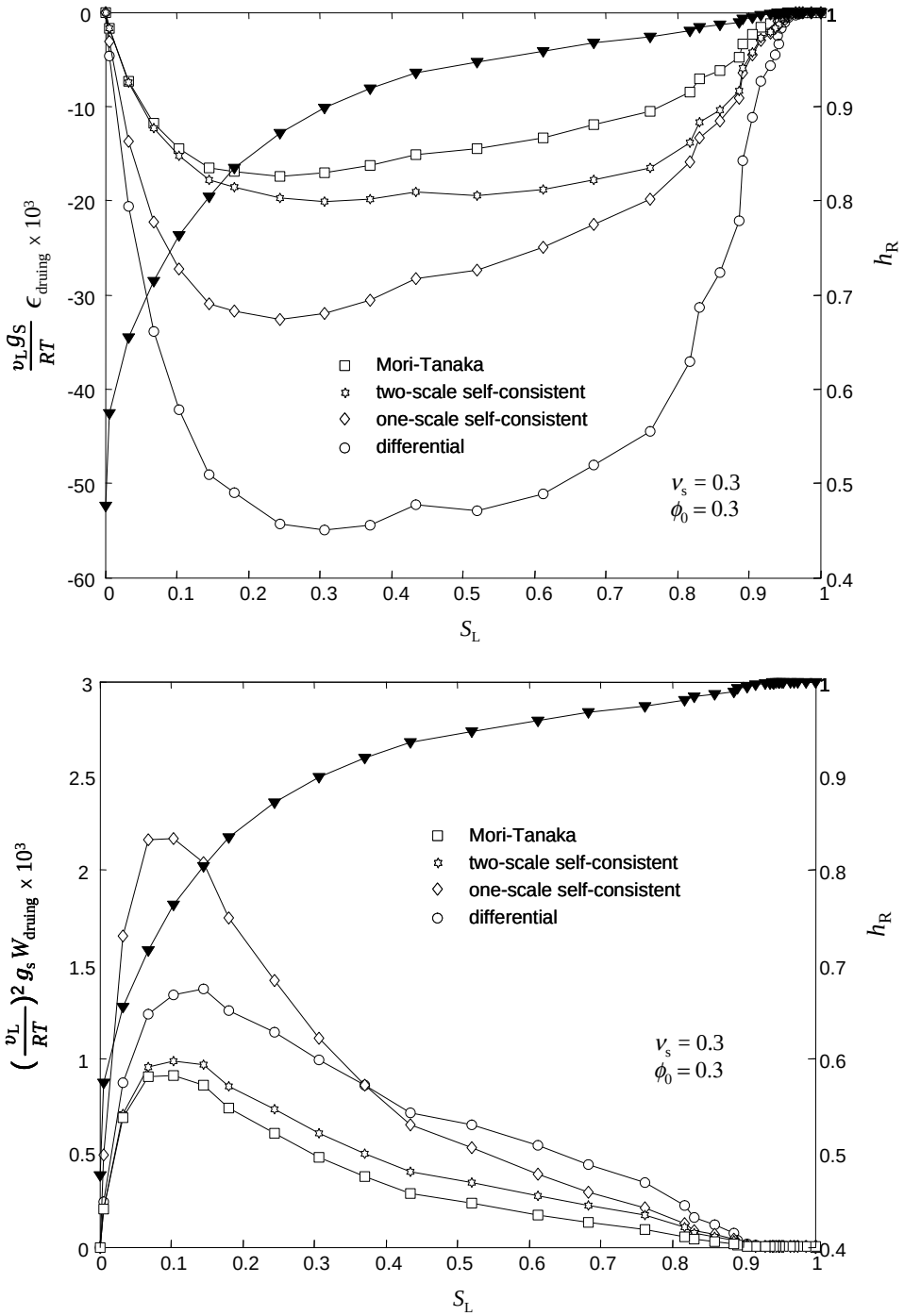

Figure 5. Normalized drying shrinkage (top) and elastic energy stored in the solid matrix during drying (bottom) versus liquid saturation, under various homogenization schemes. The cumulative volume fraction is assumed to depend on the pore entry radius as in Figure 1.

still wetted porous volume. In view of (3-4), this maximal drying shrinkage occurs when

$$\frac{p_{\mathrm{G}} - p_{\mathrm{L}}}{\chi} = -\frac{\mathrm{d}}{\mathrm{d}\chi}\left(p_{\mathrm{G}} - p_{\mathrm{L}}\right). \tag{3-5}$$

As shown in Figure 6, this condition allows the graphical determination of the capillary pressure associated with maximal drying shrinkage.

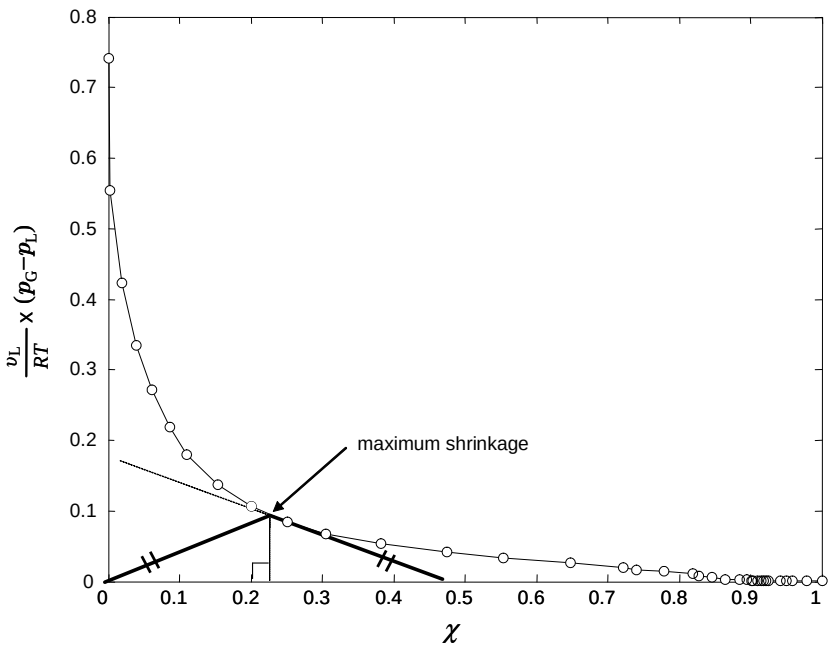

Figure 6. Graphical determination of the capillary pressure associated with maximal drying shrinkage under the differential homogenization scheme. The cumulative volume fraction is assumed to depend on the pore entry radius as in Figure 1.

As seen in the top half of Figure 5 the drying shrinkage predicted with the two-scale self-consistent scheme is less significant than the one predicted with the one-scale self-consistent scheme. Actually the bulk modulus K is the same for the two schemes while b_{L} is smaller for the two-scale self-consistent scheme (see Figure 7). In the bottom half of Figure 5 we see that the homogenization scheme affects significantly the elastic energy stored in the solid matrix during the drying process. As a result the difference of deformation of pores having a different size can significantly affects the strength of a porous material subjected to drying if its fracture is brittle and governed by a threshold in the stored elastic energy.

4. Discussion

The preceding results show that different homogenization schemes can dramatically affect the numerical values of macroscopic shrinkage and the elastic energy stored in the material. The strength of a porous material subjected to drying (if its fracture is brittle, and governed by a threshold in stored elastic energy)

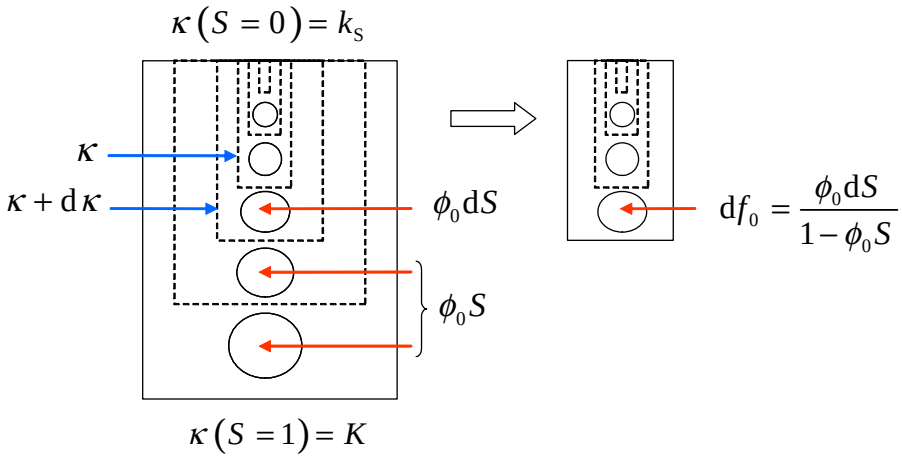

Figure 7. Sketch of the differential homogenization scheme for determining unsaturated poroelastic properties.

could therefore be significantly affected as well. This should not come as a surprise, since the choice of a homogenization scheme is already paramount to the values of the effective moduli of a composite medium. Whether neglecting pore size distribution leads to an over- or underestimation of macroscopic shrinkage is not clear, as can be seen in Figure 5; in fact, the numerical values found in the present study should not be taken for granted.

Indeed, it should be emphasized that the pore-size distribution has only been taken into account very crudely in this paper, and the assumption has been made that scale separation prevails between gas- and liquid-filled pores, *at each stage of the drying process* (i.e., for all values of liquid saturation). This strong assumption cannot be true of a continuous pore size distribution, since, as already stated, the largest liquid-filled pores are of size comparable with the smallest gas-filled pores. Even if the experimental data used in this paper (Figure 1) only imply continuity of the pore entry radii distribution (not the pore-size distribution), it is in fact well-known that the pore-size distribution is indeed continuous in cementitious materials, which effectively rules out our assumption.

Finally, it might be rightly argued that some of the homogenization schemes presented here were used outside their well-documented range of applicability. Although both the Mori–Tanaka and the differential schemes were designed for composites with bound inclusions as considered here, the self-consistent estimate is usually associated with polycrystals [Kröner 1977]; the application of this scheme to cementitious materials should therefore be considered with care. Regarding the differential scheme, as has been argued elsewhere [Norris 1985], the pore-size distribution implicitly taken into account is that of a large number of well separated families of spherical pores, which is not in contradiction with the assumption made previously, but for the fact that the basic differential scheme used here requires each family of pores to represent the same volume fraction.

The situation clearly calls for a clarification of the subtle effects of the pore-size distribution on the macroscopic properties of a porous medium. Although some attempts have been made towards this end [Bilger et al. 2007], this is still, to the authors' knowledge, an open question.

5. Concluding remarks

Unsaturated poroelasticity and homogenization schemes have been combined to reveal the effects of nonuniform pore deformation upon the mechanical behaviour of a porous material subjected to drying. This analysis can easily be extended to other confined phase transitions such as freezing [Coussy 2005; Coussy and Monteiro 2007] or drying-induced crystallization of sea salts [Coussy 2006].

However, the present analysis is based upon the assumption that scale separation prevails between the liquid- and gas-invaded pores. This assumption is in contradiction with the fact that the size of the largest pores occupied by the liquid is comparable with the size of the smallest pores occupied by the gas. This study should therefore only be considered as a first attempt at taking the pore-size distribution into account for the estimation of macroscopic shrinkage. The reliability of this estimate would greatly benefit from an upscaling method explicitly integrating pore-size distribution.

In addition, the internal stresses generated by the drying process might induce progressive cracking of the solid matrix. This in turn could significantly alter the conclusions drawn from a reversible, poroelastic, analysis. Further research is thereby needed to assess the effects of the size of the pores upon the ultimate strength of porous materials subjected to confined phase transitions, microporomechanics [Dormieux et al. 2006b] being the appropriate tool for this issue.

References

[Baroghel-Bouny et al. 1999] V. Baroghel-Bouny, M. Mainguy, T. Lassabatère, and O. Coussy, "Characterization and identification of equilibrium and transfer moisture properties for ordinary and high-performance cementitious materials", *Cement Concrete Res.* **29**:8 (1999), 1225–1238.

[Bazant and Wittmann 1982] Z. Bazant and F. Wittmann (editors), *Mathematical modeling of creep and shrinkage of concrete*, Wiley, New York, 1982.

[Bilger et al. 2007] N. Bilger, F. Auslender, M. Bornert, H. Moulinec, and A. Zaoui, "Bounds and estimates for the effective yield surface of porous media with a uniform or a nonuniform distribution of voids", *Eur. J. Mech. A Solids* **26**:5 (2007), 810–836.

[Bishop and Blight 1963] A. W. Bishop and G. E. Blight, "Some aspects of effective stress in saturated and partly saturated soils", *Géotechnique* **13** (1963), 177–197.

[Chateau and Dormieux 2002] X. Chateau and L. Dormieux, "Micromechanics of saturated and unsaturated porous media", *Int. J. Numer. Anal. Methods Geomech.* **26**:8 (2002), 831–844.

[Chateau et al. 2003] X. Chateau, L. Dormieux, and Y. Xu, "Influence of geometry changes on drying-induced strains in a cracked solid", *C. R. Mécanique* **331**:10 (2003), 679–686.

[Chertkov 2002] V. Y. Chertkov, "Modelling cracking stages of saturated soils as they dry and shrink", *Eur. J. Soil Sci.* **53**:1 (2002), 105–118.

[Coussy 1991] O. Coussy, *Mécanique des milieux poreux*, Technip, Paris, 1991. In French; translated as *Mechanics of porous continua*, Wiley, New York, 1995.

[Coussy 2004] O. Coussy, *Poromechanics*, Wiley, Chichester, 2004.

[Coussy 2005] O. Coussy, "Poromechanics of freezing materials", *J. Mech. Phys. Solids* **53**:8 (2005), 1689–1718.

[Coussy 2006] O. Coussy, "Deformation and stress from in-pore drying-induced crystallization of salt", *J. Mech. Phys. Solids* **54**:8 (2006), 1517–1547.

[Coussy 2007] O. Coussy, "Revisiting the constitutive equations of unsaturated porous solids using a Lagrangian saturation concept", *Int. J. Numer. Anal. Methods Geomech.* **31**:15 (2007), 1675–1694.

[Coussy and Monteiro 2007] O. Coussy and P. Monteiro, "Unsaturated poroelasticity for crystallization in pores", *Comput. Geotech.* **34**:4 (2007), 279–290.

[Coussy et al. 1998] O. Coussy, R. Eymard, and T. Lassabatère, "Constitutive modeling of unsaturated drying deformable materials", *J. Eng. Mech.* (*ASCE*) **124**:6 (1998), 658–667.

[Dormieux et al. 2006a] L. Dormieux, D. Kondo, and F.-J. Ulm, *Microporomechanics*, Wiley, Chichester, 2006.

[Dormieux et al. 2006b] L. Dormieux, J. Sanahuja, and S. Maghous, "Influence of capillary effects on strength of non-saturated porous media", *C. R. Mécanique* **334**:1 (2006), 19–24.

[Gusnard and Kirschner 1977] D. Gusnard and R. H. Kirschner, "Cell and organelle shrinkage during preparation for scanning electron-microscopy: effects of fixation, dehydration and critical-point drying", *J. Microsc.* **110** (1977), 51–57.

[Huang and Feldman 1985] C.-y. Huang and R. F. Feldman, "Dependence of frost resistance on the pore structure of mortar containing silica fume", *ACI J.* **82**:5 (1985), 740–743.

[Hutter et al. 1999] K. L. Hutter, L. Laloui, and L. Vulliet, "Thermodynamically based mixture models of saturated and unsaturated soils", *Mech. Cohes. Frict. Mater.* **4**:4 (1999), 295–338.

[Kozlowski and Pallardy 2002] T. T. Kozlowski and S. G. Pallardy, "Acclimation and adaptive responses of woody plants to environmental stresses", *Bot. Rev.* **68**:2 (2002), 270–334.

[Kröner 1977] E. Kröner, "Bounds for effective elastic moduli of disordered materials", *J. Mech. Phys. Solids* **25**:2 (1977), 137–155.

[Lewis and Schrefler 1998] R. W. Lewis and B. A. Schrefler, *The finite element method in the static and dynamic deformation and consolidation of porous media*, 2nd ed., Wiley, Chichester, 1998.

[Mainguy et al. 2001] M. Mainguy, O. Coussy, and V. Baroghel-Bouny, "Role of air pressure in drying of weakly permeable materials", *J. Eng. Mech.* (*ASCE*) **127**:6 (2001), 582–592.

[Norris 1985] A. N. Norris, "A differential scheme for the effective moduli of composites", *Mech. Mater.* **4**:1 (1985), 1–16.

[Ratti 1994] C. Ratti, "Shrinkage during drying of foodstuffs", *J. Food Eng.* **23**:1 (1994), 91–105.

[Santos 2000] J. A. Santos, "Mechanical behaviour of Eucalyptus wood modified by heat", *Wood Sci. Technol.* **34**:1 (2000), 39–43.

[Smith et al. 1995] D. M. Smith, G. W. Scherer, and J. M. Anderson, "Shrinkage during drying of silica gel", *J. Non-Cryst. Solids* **188**:3 (1995), 191–206.

Received 14 Dec 2007. Accepted 8 Nov 2008.

OLIVIER P. COUSSY: Olivier.Coussy@mail.enpc.fr
Université Paris-Est, UR Navier, École des Ponts, 6-8 Av. Blaise Pascal, Cité Descartes, F-77455 Marne-la-Vallée Cedex 2, France

SÉBASTIEN BRISARD: Sebastien.Brisard@mail.enpc.fr
Université Paris-Est, UR Navier, École des Ponts, 6-8 Av. Blaise Pascal, Cité Descartes, F-77455 Marne-la-Vallée Cedex 2, France